


 Cite this: *Chem. Commun.*, 2024, 60, 7737

 Received 30th April 2024,  
 Accepted 27th June 2024

DOI: 10.1039/d4cc02086c

[rsc.li/chemcomm](https://rsc.li/chemcomm)

# A novel and simple method yields highly dispersed Au/TS-1 catalysts for enhanced propylene hydro-oxidation†

 Zhihua Zhang, Jialun Xu, Kesheng Xu, Yuxia Zhong, Shudong Shi, Xuezhi Duan \* and Xinggui Zhou\*

**We demonstrate a simple method for preparing highly active Au/TS-1 catalysts for propylene hydro-oxidation, which involves sequentially impregnating HAuCl<sub>4</sub> and Cs<sub>2</sub>CO<sub>3</sub> solutions onto TS-1. The Au/TS-1 catalysts synthesized by this method exhibit high Au uptake efficiency (~100%), high dispersion of Au nanoparticles and superior activity.**

The direct gas phase epoxidation of propylene with O<sub>2</sub> and H<sub>2</sub> to produce propylene oxide (PO), simplified as the HOPO process, has significant advantages, such as simplicity, environmentally friendliness, high selectivity and cost-efficiency, and has attracted growing interest.<sup>1,2</sup> Currently, nano Au particles supported on a titanium silicalite-1 (*e.g.*, TS-1) catalyst are the most widely used catalyst for the HOPO reaction.<sup>3,4</sup> O<sub>2</sub> and H<sub>2</sub> first react on the surface of the Au nanoparticles to generate hydro-peroxide species, which then migrate to the isolated Ti<sup>4+</sup> sites in TS-1 to form Ti-OOH intermediates that catalyse propylene to PO consequently.<sup>5,6</sup> That is to say, the Au/TS-1 catalyst is a bifunctional catalyst. From a geometric point of view, the catalytic performance of Au/TS-1 is significantly affected by Au particle size, and small Au nanoparticles generally exhibit superior activity.<sup>7,8</sup> Current works suggest that gold clusters immobilized within the micropores of TS-1 are the primary active sites.<sup>9,10</sup>

Generally, the size of Au nanoparticles is greatly influenced by the catalyst preparation method.<sup>11</sup> The impregnation method is one of the mostly used catalyst preparation methods, which has the advantages of simplicity, and high uptake efficiency of the precursor.<sup>11</sup> Previous literature has found that Au catalysts prepared by impregnating HAuCl<sub>4</sub> onto titanium-containing materials form large Au nanoparticles due to the high content of residual chloride ion, which can promote the

agglomeration of Au particles during the activation process, thus resulting in low activity.<sup>12</sup> The deposition-precipitation method (*i.e.*, DP method) can effectively produce gold precursors (*i.e.*, [AuCl<sub>x</sub>(OH)<sub>4-x</sub>]<sup>-</sup>) with less chloride ions by the hydrolysis reaction between hydroxide ions and chloroaurate anions.<sup>3,7</sup> As a result, the Au/TS-1 catalysts prepared by the DP method show a relatively narrower size distribution of Au particles, which has become the mostly used method for preparing highly active Au-Ti bifunctional catalysts.<sup>11</sup> However, the gold uptake efficiency is relatively low (<5%), and the catalytic performance of the Au/TS-1 catalyst prepared by this method is highly sensitive to many preparation parameters (*e.g.*, pH, temperature), which may be the key factors that hinder the scale-up production of highly efficient Au/TS-1 catalysts.<sup>3,4</sup>

Based on the mechanism of the DP method and the advantage of high gold uptake efficiency of the incipient wetness impregnation method (*i.e.*, IWI method), we propose a strategy for the preparation of highly active Au/TS-1 catalysts by a modified incipient wetness impregnation method (denoted as m-IWI method): the HAuCl<sub>4</sub> is firstly impregnated onto TS-1, followed by impregnation of an alkaline solution to promote the hydrolysis of AuCl<sub>4</sub><sup>-</sup>, thereby reducing the content of chloride ion. In addition, we also prepared Au/TS-1 catalysts by the IWI method and DP method as reference catalysts for comparative studies, aiming at establishing a reliable structure-performance relationship. FT-IR spectra (Fig. S1, ESI†) show that the catalyst preparation method shows negligible influence on the Ti environment, MFI structure and hydrophobicity of the three Au/TS-1 catalysts, which is confirmed by the similar intensities of the bands at 550 cm<sup>-1</sup> (vibration of double five-membered ring unit), 960 cm<sup>-1</sup> (stretching of Ti-O-Si band) and 3420 cm<sup>-1</sup> (vibrations of hydrogen-bonded silanols).<sup>13,14</sup> This is also in agreement with the similar Ti<sub>2p</sub> and Si<sub>2p</sub> binding energies over the three catalysts (Fig. S2, ESI†).

The Au loadings and Au uptake efficiency of the Au/TS-1 catalysts prepared by different methods are shown in Table S1 (ESI†). As

State Key Laboratory of Chemical Engineering, East China University of Science and Technology, 130 Meilong Road, Shanghai 200237, China.

E-mail: xzduan@ecust.edu.cn; Fax: +86-21-64253528

† Electronic supplementary information (ESI) available. See DOI: <https://doi.org/10.1039/d4cc02086c>

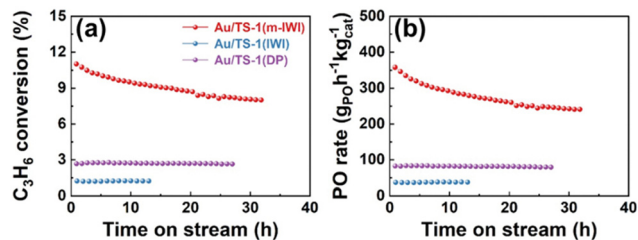


Fig. 1 (a) Conversion of propylene and (b) PO formation rate of the 0.10 wt% Au/TS-1 catalysts prepared by different methods. Reaction temperature: 190 °C, C<sub>3</sub>H<sub>6</sub> concentration: 10% vol.

shown, the gold uptake efficiency is close to 100% for the 0.10 wt% Au/TS-1(m-IWI) catalyst prepared by the m-IWI method, much higher than that of the 0.10 wt% Au/TS-1 (DP) catalyst (*ca.* 2.2%) prepared by the DP method. The activity of the Au/TS-1 catalysts prepared by different methods is shown in Fig. 1. As shown, though the three Au/TS-1 catalysts have similar Au loadings (*ca.* 0.10 wt%, shown in Table S1, ESI<sup>†</sup>), the propylene conversion of the 0.1 wt% Au/TS-1(m-IWI) catalyst exceeds 10% (Fig. 1a), and the initial PO formation rate is as high as 358 g<sub>PO</sub> h<sup>-1</sup> kg<sub>cat</sub><sup>-1</sup> (Fig. 1b), which is much higher than that of the catalysts prepared by the DP method (97 g<sub>PO</sub> h<sup>-1</sup> kg<sub>cat</sub><sup>-1</sup>) and the IWI method (48 g<sub>PO</sub> h<sup>-1</sup> kg<sub>cat</sub><sup>-1</sup>). Moreover, the 0.1 wt% Au/TS-1(m-IWI) catalyst also displays high selectivity (Fig. S3a, ESI<sup>†</sup>) and hydrogen utilization efficiency (*i.e.*, hydrogen efficiency, shown in Fig. S3b, ESI<sup>†</sup>) compared to the catalyst prepared by the DP method, though the conversion of the former is much higher than that of the latter, as well as the 0.10 wt% Au/TS-1(IWI) catalyst prepared by the IWI method using chloroauric acid as a gold precursor.

To explore the reasons for the superior catalytic performance of the 0.10 wt% Au/TS-1(m-IWI) catalyst, HAADF-STEM was then employed to analyze the Au size distribution in the Au/TS-1 catalysts prepared by different methods, and the results are shown in Fig. S4 (ESI<sup>†</sup>). As shown, the average size of the Au nanoparticles in the 0.10 wt% Au/TS-1(m-IWI) catalyst (*ca.* 2.4 nm) is similar to that of the 0.10 wt% Au/TS-1(DP) catalyst (*ca.* 2.7 nm). However, the size distribution of Au nanoparticles in the former is narrower than in the latter. Additionally, the size distribution of Au nanoparticles in the 0.10 wt% Au/TS-1(IWI) catalyst is very broad, and a number of large particles can be clearly observed, thus showing poor activity. Therefore, compared to the DP method and IWI method, the m-IWI method shows the advantage of synthesizing a Au/TS-1 catalyst with narrow Au size distribution, which is the main reason for the superior activity of the 0.10 wt% Au/TS-1(IWI) catalyst.

Notably, as shown in Fig. S4 (ESI<sup>†</sup>), the average Au particle size of the 0.10 wt% Au/TS-1 (m-IWI) catalysts prepared by the m-IWI method and DP method are similar. However, the PO formation rate of the former is approximately 3.9 times higher than that of the latter. Therefore, we speculate that a number of tiny Au clusters may exist in the 0.10 wt% Au/TS-1(m-IWI) catalyst, which is difficult to be detected by HAADF-STEM (detection limit  $\sim$  1 nm). Consequently, aberration-corrected

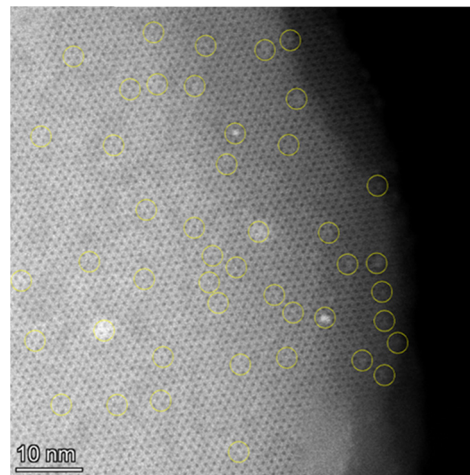
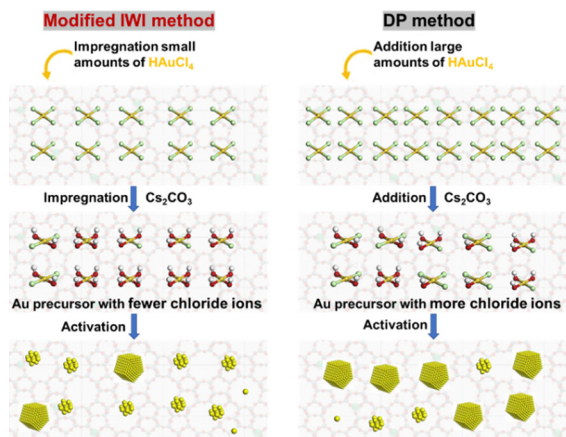


Fig. 2 Cs-corrected STEM image of the 0.10 wt% Au/TS-1(m-IWI) catalyst.

electron microscopy was used to characterize the Au nanoparticles on the 0.10 wt% Au/TS-1(m-IWI) catalyst, and the results are shown in Fig. 2. It can be seen that many tiny Au clusters with a size of about 0.5–1 nm are indeed present on the surface of the 0.10 wt% Au/TS-1(m-IWI) catalyst. In addition to the tiny Au clusters, a few gold single-atoms can also be observed on this catalyst. To understand the contribution of tiny Au clusters and gold single atoms for PO formation, we further reduced the gold loading and prepared 0.01 wt% and 0.05 wt% Au/TS-1(m-IWI) catalysts by the m-IWI method, and their activities are shown in Fig. S5 (ESI<sup>†</sup>). It can be seen that the PO formation rate of the 0.05 wt% Au/TS-1(m-IWI) catalyst is *ca.* 5 times higher than that of the 0.01 wt% Au/TS-1(m-IWI) catalyst, and the activity of the former calculated on the basis of per-mass-of-gold is the same as that of the 0.01 wt% Au/TS-1 (m-IWI) catalyst, indicating that the two catalysts have the same Au active sites. Considering that increasing the gold loading of the Au/TS-1 catalyst usually leads to inferior dispersion of Au nanoparticles, more Au clusters or particles rather than single-atom Au would exist on the Au/TS-1 catalyst with high gold loading. Therefore, based on the results of aberration-corrected electron microscopy (Fig. 2) and the catalytic performance of the 0.01 wt% and 0.05 wt% Au/TS-1(m-IWI) catalysts, we infer that the tiny gold clusters on the 0.10 wt% Au/TS-1(m-IWI) catalyst contribute significantly to the activity. Moreover, the peak intensity of Au 4f over the Au/TS-1 (m-IWI) catalyst is much weaker than that of the Au/TS-1 (IWI) and Au/TS-1 (DP) catalysts. Thereby, it is reasonable to postulate that the majority of Au clusters in the Au/TS-1 (m-IWI) catalyst are located in the micropores of TS-1.

Based on the above results, we have proposed the following strategy for the preparation of highly active Au/TS-1 catalysts by the m-IWI method (shown in Scheme 1): most of the AuCl<sub>4</sub><sup>-</sup> will strongly adsorb on the surface of TS-1 when HAuCl<sub>4</sub> is impregnated into TS-1, as the pH (*ca.* 2.7) of the HAuCl<sub>4</sub> solution is close to the isoelectric point of TS-1 (*ca.* 2 and 3). Subsequently, the AuCl<sub>4</sub><sup>-</sup> will gradually hydrolyse after impregnating Cs<sub>2</sub>CO<sub>3</sub> solution to form a



Scheme 1 Possible pathway for the preparation of Au/TS-1 catalysts by the modified IWI method and DP method.

$[\text{AuCl}_x(\text{OH})_{4-x}]^-$  complex with less chlorine.<sup>7</sup> Contrary to the DP method that requires addition of large amounts of  $\text{H}_2\text{O}$  (ca. 44 mL  $\text{H}_2\text{O}$  per  $\text{g}_{\text{TS-1}}$ ) during the preparation process, the modified incipient wetness impregnation method forgoes the need for additional water and involves smaller amounts (0.8 mL  $\text{g}_{\text{TS-1}}^{-1}$ ) of solution. As a result, the pH of the solution absorbed on the surface of TS-1 is relatively higher during the impregnation of  $\text{CS}_2\text{CO}_3$  solution, which is beneficial to hydrolysing  $\text{AuCl}_4^-$ , thus forming adsorbed Au species with fewer chloride ions. In this way, the catalysts prepared by the m-IWI method give a narrower Au size distribution and form a number of tiny Au clusters. Additionally, the pH of the slurry (7.5–8.3) is higher than the isoelectric point of TS-1 (2 and 3) during the DP process.<sup>7</sup> Therefore, to achieve a comparatively high gold loading, large amounts of  $\text{HAuCl}_4$  are added with the aim of ensuring that a sufficient number of negatively charged  $[\text{AuCl}_x(\text{OH})_{4-x}]^-$  are available for adsorption onto the negatively charged surface of TS-1, thus leading to a lower Au uptake efficiency compared with the m-IWI method.

Optimizing the catalytic performance of the Au/TS-1 catalyst synthesized by the m-IWI method is also conducted. Fig. S6 (ESI<sup>†</sup>) shows the effect of propylene concentration on the catalytic performance. It can be observed that when the propylene concentration increases from 10% to 20%, the PO formation rate further improved to  $417 \text{ g}_{\text{PO}} \text{ h}^{-1} \text{ kg}_{\text{cat}}^{-1}$ , and the PO selectivity and hydrogen efficiency are also improved. Furthermore, increasing the concentration of propylene is also beneficial to reducing the selectivity of the by-products, especially for  $\text{CO}_2$  (Fig. S7, ESI<sup>†</sup>). Taking into account the competitive adsorption between propylene and PO on the  $\text{Ti}^{4+}$  sites,<sup>15,16</sup> increasing the concentration of propylene will promote the desorption of PO, which is beneficial for providing more active sites for the epoxidation and also inhibiting the isomerization and deep oxidation of PO. Therefore, the PO formation rate, selectivity and hydrogen efficiency increase with the increase of the propylene concentration.<sup>16</sup>

Fig. S8 (ESI<sup>†</sup>) shows the effect of reaction temperature on the catalytic performance. As shown, both the conversion of

propylene and PO formation rate increase with the increase of the reaction temperature, while the PO selectivity and hydrogen efficiency show an opposite trend. Notably, the hydrogen efficiency seems to be more sensitive to the reaction temperature, which is due to the significantly enhanced decomposition of hydro-peroxide species at high reaction temperature, thus reducing the hydrogen efficiency.<sup>17</sup> Notably, the PO formation rate significantly increased with the increase of the reaction temperature in the range of 160–180 °C. However, the increase in the formation rate of PO decelerates with further increase of the reaction temperature, which may be due to the ring-opening of PO to by-products.<sup>15,17</sup> Additionally, the PO formation rate on the 0.10 wt% Au/TS-1(m-IWI) catalyst is ca.  $250 \text{ g}_{\text{PO}} \text{ h}^{-1} \text{ kg}_{\text{cat}}^{-1}$  at 170 °C, while a high PO selectivity (95.7%) and hydrogen efficiency (34%) could also be maintained, better than the reported Au/TS-1 catalysts with the same gold loading (ca. 0.10 wt%).<sup>4</sup>

Fig. S9 (ESI<sup>†</sup>) shows the influence of gold loadings on the catalytic performance. As shown, the conversion of  $\text{C}_3\text{H}_6$  and PO formation rate increase with the increase of gold loading, and the PO selectivity changes slightly with the increase of gold loading, while the hydrogen efficiency decreases significantly with the increase of the gold loading. Notably, even for the Au/TS-1(m-IWI) catalyst with a gold loading as low as 0.05 wt%, the PO formation rate is still relatively high (ca.  $326 \text{ g}_{\text{PO}} \text{ h}^{-1} \text{ kg}_{\text{cat}}^{-1}$ ), approaching the activity of reported Au/TS-1 catalysts with high Au loadings (>0.3 wt%).<sup>4,18</sup> This may be attributed to the fact that the m-IWI method facilitates the formation of highly active tiny Au clusters, thus exhibiting excellent activity even at low gold loading.

Table 1 gives a comparison of the catalytic performance between Au/TS-1(m-IWI) catalysts and various Au-Ti bifunctional catalysts taken from the literature. Clearly, the 0.10 wt% Au/TS-1(m-IWI) catalyst exhibits a PO formation rate 1.7 times higher than that of the reported Au/TS-1 catalyst with similar gold loading, while the former shows higher selectivity towards PO and hydrogen efficiency. Additionally, it is worth noting that the PO formation rate on the 0.05 wt% Au/TS-1(m-IWI) catalyst is about 3 times higher than that of the 0.05 wt% Au/TS-1 catalyst reported in the literature; meanwhile, this catalyst displays higher selectivity and hydrogen efficiency.<sup>4</sup> Moreover,

Table 1 Catalytic performance of various Au-Ti bifunctional catalysts

Catalyst	PO rate ( $\text{g}_{\text{PO}} \text{ h}^{-1} \text{ kg}_{\text{cat}}^{-1}$ )	Sel. (%)	$\text{H}_2$ eff. (%)	Ref.
0.10 wt% Au/TS-1(m-IWI) <sup>a</sup>	417	91.2	24	This work
0.05 wt% Au/TS-1(m-IWI) <sup>a</sup>	326	92.7	34	This work
0.05 wt% Au/TS-1 <sup>b</sup>	107	86.0	25	4
0.11 wt% Au/TS-1 <sup>b</sup>	246	86.4	20	
0.18 wt% Au/TS-1 <sup>b</sup>	257	86.0	19	4
0.76 wt% Au/TS-1 <sup>b</sup>	315	79.0	19	4
0.12 wt% Au/TS-1 <sup>b</sup>	250	92.5	30	12
0.30 wt% Au/TS-1 <sup>b</sup>	335	93.0	—	18
0.65 wt% Au/TS-1 <sup>c</sup>	477	92.0	11	19

<sup>a</sup> Reaction temperature: 190 °C,  $\text{C}_3\text{H}_6$  concentration: 20% vol.

<sup>b</sup> Reaction temperature: 200 °C,  $\text{C}_3\text{H}_6$  concentration: 10% vol. <sup>c</sup> Reaction temperature: 210 °C,  $\text{C}_3\text{H}_6$  concentration: 10% vol.

the activity of the 0.05 wt% Au/TS-1(m-IWI) catalyst is also comparable to that of the reported Au/TS-1 catalysts with high gold loadings (>0.3 wt%), indicating a high utilization efficiency of Au atoms.<sup>4,18</sup> This is also beneficial for reducing the cost of Au–Ti bifunctional catalysts. Therefore, the Au–Ti bifunctional catalyst prepared by the modified incipient wetness impregnation method not only shows excellent catalytic performance and high gold uptake efficiency, but also has high Au atom utilization efficiency. The insights revealed here may pave a new way for the scale-up production of highly efficient Au–Ti bifunctional catalysts in the future.

Catalyst stability is also one of the key factors that hinders the industrial application of the HOPO process. Previous work has demonstrated that the micropores of the Au/TS-1 catalyst being blocked by coke is the main reason for the deactivation of the catalyst.<sup>13</sup> Therefore, uncalcined TS-1 (*i.e.*, TS-1-B) with micropores blocked by TPA<sup>+</sup> templates was then used to immobilize gold precursor onto the external surface of TS-1-B by the m-IWI method, aiming at obtaining good stability. The stability of the Au/TS-1-B(m-IWI) catalyst is shown in Fig. S10 (ESI<sup>†</sup>). It can be observed from Fig. S10 (ESI<sup>†</sup>) that both the 0.10 wt% Au/TS-1-B(m-IWI) and 0.05 wt% Au/TS-1-B(m-IWI) catalysts show good stability, with no significant decline in the PO formation rate observed over a period of 130 h. Additionally, the size distribution of the Au nanoparticles before and after reaction over the 0.05 wt% Au/TS-1-B(m-IWI) catalyst (shown in Fig. S11, ESI<sup>†</sup>) indicates that there is no significant aggregation of the Au nanoparticles during the long-term test, showing good stability of Au particles.

In summary, we have demonstrated that the m-IWI method, which involves impregnating HAuCl<sub>4</sub> onto TS-1 and then succeeded by adding alkaline solution to facilitate the hydrolysis of the gold precursor, can successfully prepare highly active Au/TS-1 catalysts for the HOPO reaction. Compared with the Au/TS-1 catalysts prepared by the IWI method and DP method, the as-prepared Au/TS-1 catalysts not only exhibit narrower Au size distribution but also have plenty of tiny Au clusters, as confirmed by the HAADF-STEM and aberration-corrected electron microscopy. Consequently, the PO formation rate over the 0.10 wt% Au/TS-1(m-IWI) catalyst (*ca.* 417 g<sub>PO</sub> h<sup>-1</sup> kg<sub>cat</sub><sup>-1</sup>) is *ca.* 7.0 times and 3.9 times higher than that of the 0.10 wt% Au/TS-1 catalysts prepared by the IWI method and DP method, respectively. Notably, the Au/TS-1(m-IWI) catalyst with a low gold loading (*ca.* 0.05 wt%) also shows very high PO formation rate (*ca.* 326 g<sub>PO</sub> h<sup>-1</sup> kg<sub>cat</sub><sup>-1</sup>), showing high Au atom utilization efficiency. Additionally, the m-IWI method also shows high Au uptake efficiency (*ca.* 100%). Moreover, immobilizing Au nanoparticles onto the external surface of uncalcined TS-1 by the m-IWI method also displays excellent stability (>130 h). The insights reported here will provide important guidance for the preparation of highly efficient Au–Ti bifunctional catalysts and other molecular sieve supported highly dispersed metal catalysts.

This work is financially supported by the Ministry of Science and Technology of the People's Republic of China under the Research Fund for National Key R&D Program of China (2021YFA1501403), the National Natural Science Foundation of China (22208093, 22038003, 22178100, 21922803), the Program of Shanghai Academic/Technology Research Leader (21XD1421000), the Shanghai Science and Technology Innovation Action Plan (22JC1403800), and the Innovation Program of the Shanghai Municipal Education Commission.

## Data availability

The data supporting this article have been included as part of the ESI.<sup>†</sup>

## Conflicts of interest

There are no conflicts to declare.

## Notes and references

- V.-H. Nguyen, B.-S. Nguyen, C. Hu, A. Sharma, D.-V. N. Vo, Z. Jin, M. Shokouhimehr, H. W. Jang, S. Y. Kim and Q. V. Le, *Catalysis*, 2020, **10**, 442.
- T. Ishida, T. Murayama, A. Taketoshi and M. Haruta, *Chem. Rev.*, 2019, **120**(2), 464–525.
- W.-S. Lee, M. C. Akatay, E. A. Stach, F. H. Ribeiro and W. N. Delgass, *J. Catal.*, 2012, **287**, 178–189.
- W.-S. Lee, M. C. Akatay, E. A. Stach, F. H. Ribeiro and W. N. Delgass, *J. Catal.*, 2013, **308**, 98–113.
- B. Chowdhury, J. J. Bravo-Suárez, N. Mimura, J. Lu, K. K. Bando, S. Tsubota and M. Haruta, *J. Phys. Chem. B*, 2006, **110**, 22995–22999.
- W. Du, Z. Zhang, Y. Tang, Q. Wang, N. Song, X. Duan and X. Zhou, *ACS Catal.*, 2023, **13**, 2069–2085.
- X. Feng, Z. Song, Y. Liu, X. Chen, X. Jin, W. Yan, C. Yang, J. Luo, X. Zhou and D. Chen, *ACS Catal.*, 2018, **8**, 10649–10657.
- X. Feng, X. Duan, G. Qian, X. Zhou, D. Chen and W. Yuan, *J. Catal.*, 2014, **317**, 99–104.
- W.-S. Lee, L. C. Lai, M. C. Akatay, E. A. Stach, F. H. Ribeiro and W. N. Delgass, *J. Catal.*, 2012, **296**, 31–42.
- Z. Li, J. Zhang, D. Wang, W. Ma and Q. Zhong, *J. Phys. Chem. C*, 2017, **121**, 25215–25222.
- M. Okumura, T. Fujitani, J. Huang and T. Ishida, *ACS Catal.*, 2015, **5**, 4699–4707.
- Z. Lu, J. Kunisch, Z. R. Gan, M. Bunian, T. P. Wu and Y. Lei, *ChemCatChem*, 2020, **12**, 5993–5999.
- X. Feng, X. Duan, G. Qian, X. Zhou, D. Chen and W. Yuan, *Appl. Catal., B*, 2014, **150**, 396–401.
- S. Kanungo, K. S. Keshri, E. J. M. Hensen, B. Chowdhury, J. C. Schouten and M. F. Neira d'Angelo, *Catal. Sci. Technol.*, 2018, **8**, 3052.
- G. Wang, W. Du, X. Duan, Y. Cao, Z. Zhang, J. Xu, W. Chen, G. Qian, W. Yuan, X. Zhou and D. Chen, *Chem. Catal.*, 2021, **1**(4), 885–895.
- S. Kanungo, D. M. P. Ferrandez, F. N. d'Angelo, J. C. Schouten and T. A. Nijhuis, *J. Catal.*, 2016, **338**, 284–294.
- Y. Hong, J. Huang, G. Zhan and Q. Li, *Ind. Eng. Chem. Res.*, 2019, **58**, 21953–21960.
- Q. Zhu, M. Liang, W. Yan and W. Ma, *Microporous Mesoporous Mater.*, 2019, **278**, 307–313.
- J. Peng, K. Liu, S. Guo, W. Chen, H. Hu, Q. Huang and X. Chen, *Chem. Eng. J.*, 2023, **472**, 144895.